

Polymer-metal waveguides characterization by Fourier plane leakage radiation microscopy

Cite as: Appl. Phys. Lett. **91**, 243102 (2007); <https://doi.org/10.1063/1.2824840>

Submitted: 02 October 2007 • Accepted: 24 November 2007 • Published Online: 10 December 2007

S. Massenot, J. Grandidier, A. Bouhelier, et al.



View Online



Export Citation

ARTICLES YOU MAY BE INTERESTED IN

Fourier plane imaging microscopy

Journal of Applied Physics **116**, 103102 (2014); <https://doi.org/10.1063/1.4895157>

Back focal plane imaging spectroscopy of photonic crystals

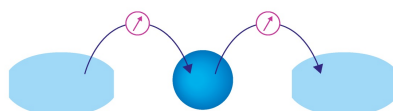
Applied Physics Letters **101**, 081904 (2012); <https://doi.org/10.1063/1.4746251>

How to erase surface plasmon fringes

Applied Physics Letters **89**, 091117 (2006); <https://doi.org/10.1063/1.2339043>

Webinar

Interfaces: how they make
or break a nanodevice



March 29th – Register now



Zurich
Instruments

AIP
Publishing

Appl. Phys. Lett. **91**, 243102 (2007); <https://doi.org/10.1063/1.2824840>

91, 243102

© 2007 American Institute of Physics.

Polymer-metal waveguides characterization by Fourier plane leakage radiation microscopy

S. Massenot,^{a)} J. Grandidier, A. Bouhelier, G. Colas des Francs, L. Markey, J.-C. Weeber, and A. Dereux

Institut Carnot de Bourgogne, UMR 5209 CNRS-Université de Bourgogne, 9 Av. A. Savary, BP 47 870, F-21078 Dijon Cedex, France

J. Renger, M. U. González, and R. Quidant

ICFO-Institut de Ciències Fotòniques, Castelldefels 08860 Barcelona, Spain

(Received 2 October 2007; accepted 24 November 2007; published online 10 December 2007)

The guiding properties of polymer waveguides on a thin gold film are investigated in the optical regime. The details of propagation in the waveguides are studied simultaneously in the object and Fourier planes, providing direct measurement of both the real and imaginary parts of the effective index of the guided mode. A fair agreement between theoretical analysis provided by the differential method and experimental leakage radiation microscopy data is shown. All these tools bring valuable information for designing and understanding such devices. © 2007 American Institute of Physics. [DOI: 10.1063/1.2824840]

Due to their high bandwidth, integrated optical components have raised considerable interests in the race to overcome data transfer limitation in electronic circuits. For instance, interconnections between chips realized in the optical domain could significantly increase their bit rate. Among the different existing optical waveguiding technologies, polymeric elements lying on a metal film offer a number of advantages. On the one hand, they dispose of a high index contrast required for large scale integration and, on the other hand, the presence of a metal layer let foresee the possibility to develop plasmonic components, which present interesting properties such as field confinement and exaltation at dielectric/metal interfaces.¹ Compared to silicon-on-insulator technology, these waveguides are intrinsically lossy. However, they are still of interest when propagation lengths involved are short, typically a few tens of micrometers. It is notably true in the near-infrared domain, i.e., standard telecommunications spectral bands, where the losses associated with noble metal substrates are relatively low.

The integration of polymer onboard interconnects requires the understanding and optimization of light propagation in basic structures such as the straight waveguide. Such structures were theoretically investigated by the effective index model and by finite elements analysis, in particular for structures supporting plasmon modes.^{2,3} Propagation losses of 0.1 dB/ μm have been calculated for a wavelength of 1550 nm and the preliminary guiding demonstration was experimentally observed on metal/polymer structure⁴ (for $\lambda = 632.8$ nm). Closely related, SiO₂ dielectric waveguides (straight and bent) have also been investigated and propagation lengths versus bent radii were characterized^{5,6} (for $\lambda = 800$ nm). However, the use of polymer waveguides instead of SiO₂ brings additional advantages. The polymers are widely accessible, presenting a variety of chemical and optical specificities, sensibilities, and dopings. The latter feature can be of importance in the development of active and dynamic functionalities (modulators or switches, for example) addressed either optically or electrically.

The recent interest for dielectric elements on metal films increases the need of powerful design and characterization techniques and it is the aim of this letter to present suitable tools. The structures are modeled using the differential method, which is particularly suited in the investigation of this kind of waveguide since it calculates the field inside and outside the waveguide and provides the complex effective index of the guided mode. The characteristics of the waveguides are experimentally measured by direct and Fourier plane leakage radiation microscopy.^{7–10} This dual-plane imaging technique allows to retrieve the real and imaginary parts of the effective index of the supported modes without requiring advanced scanning near-field imaging techniques¹¹ or mode profiling of the output end.

The geometry of the structure is schematically shown in Fig. 1. It consists of a polymer waveguide composed of polymethylmethacrylate (PMMA) (refractive index n_w) deposited on a gold metal layer (50 nm thick, refractive index n_m) lying on a glass substrate (refractive index n_1). The waveguide is illuminated from the substrate with a plane wave or a Gaussian beam with an angle of incidence θ and an azimuth δ . $\delta = 90^\circ$ corresponds to an incident wavevector parallel to the longitudinal axis of the waveguide.

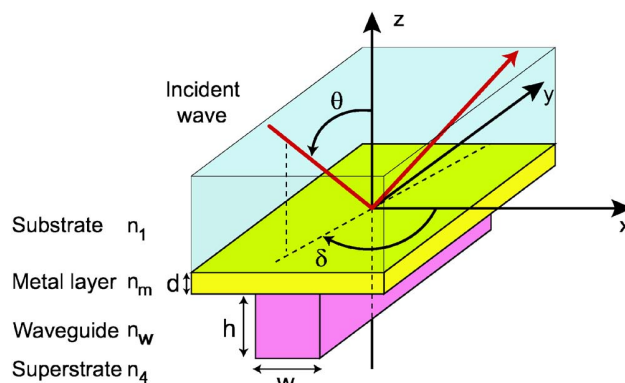


FIG. 1. (Color online) Sketch of the polymer waveguide studied and associated notations.

^{a)}Electronic mail: sebastien.massenot@u-bourgogne.fr.

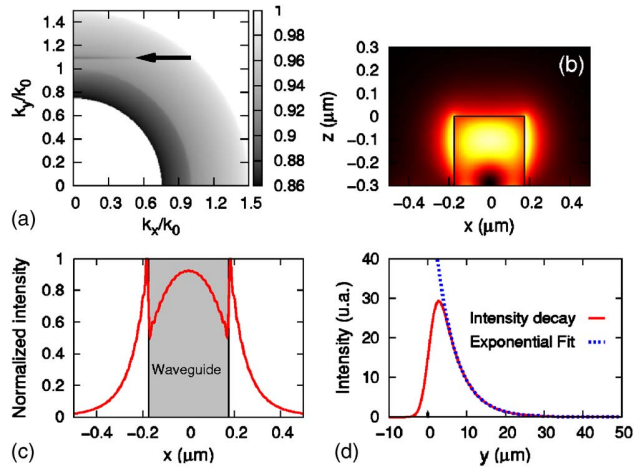


FIG. 2. (Color online) (a) Fourier plane (reflectivity map of the structure) for a TE polarized incident plane wave. (b) Normalized intensity profile of the TE mode supported by the structure. (c) Mode profile at $z = -0.1 \mu\text{m}$. (d) Calculated intensity distribution along the longitudinal axis.

The excitation condition of a guided mode in the structure is given by the phase matching condition:¹² $k_0 n_1 \sin \theta \sin \delta = \Re(\beta) = k_0 \Re(n_{\text{eff}})$ (1), where k_0 is the free-space wavevector, β the propagation constant of the considered guided mode, and n_{eff} , its associated complex effective index ($n_{\text{eff}} = \nu + i\alpha$). The real part of n_{eff} is used in Eq. 1 because of the presence of the metal layer which is a source of Ohmic and radiative losses. The propagation length of the mode, corresponding to the attenuation of the intensity at $1/e$, is defined by $L_\alpha = \lambda_0 / 4\pi\alpha$, where λ_0 is the wavelength in vacuum.

This waveguide structure is theoretically analyzed using the differential method,¹³ originally dedicated to the study of diffraction gratings. It is relatively easy to extend this method to a nonperiodic structure by avoiding coupling effects between the periodic units and considering a grating period much larger than the typical lateral extension of the mode supported by the system of interest. A scattering matrix algorithm helps to propagate in the different layers of the structure without numerical instabilities.¹⁴ By using angular spectrum decomposition, it is possible to extend the calculation to arbitrary excitation profiles.¹⁵

Following notations of Fig. 1, the parameters of the considered waveguide are $n_1 = 1.5$, $n_w = 1.493$, $n_4 = 1.0$, $d = 50 \text{ nm}$, $h = 300 \text{ nm}$, $w = 350 \text{ nm}$, and $\lambda = 632.8 \text{ nm}$. The refractive index of gold n_m is calculated from Ref. 16 with piecewise cubic Hermite interpolation. By analyzing the reflectivity of this structure for all the angles θ and δ , Fourier planes can be established (they contain the spatial information associated to the angular response of the structure). Figure 2(a) shows the reflectivity map calculated over $30^\circ < \theta < 89^\circ$ and $0^\circ < \delta < 90^\circ$ for TE incident plane waves. The darker areas in Fig. 2(a) are regions of lower reflectivity. A horizontal dark fringe is observed, that corresponds to a constant value of the k_y component of the incident wave. Following Eq. (1), this line can be interpreted as being the signature of a guided mode in the structure. The position of the line gives a direct measure of the real part of the mode effective index, here $\nu = 1.095$. The single mode operation is confirmed by Figs. 2(b) and 2(c) showing the calculated distribution of intensity across the waveguide. To estimate the propagation length of the mode, the evolution of the intensity

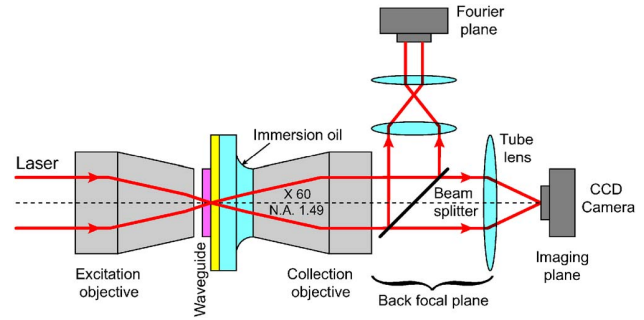


FIG. 3. (Color online) Principle of leakage radiation microscopy.

along the waveguide is calculated by replacing the plane wave illumination by a Gaussian excitation. Figure 2(d) shows an exponential decay of the intensity with a characteristic length $L_\alpha = 5.2 \mu\text{m}$.

To experimentally verify the theoretical values of the complex effective index of the guided mode, polymer waveguides were fabricated on a 50-nm-thick gold layer using standard electron-beam lithography and the size parameters were those used in the calculations.

The waveguide was optically characterized by leakage radiation microscopy.^{7,8,17} This method uses optical index matching through a high-numerical aperture lens to collect radiation losses occurring in the waveguide during propagation. These losses are mainly emitted into the substrate through the gold layer. Imaging this leakage radiation gives valuable information of the guided mode structure. A schematic of the setup is shown in Fig. 3. Depending on where leakage radiations are detected on the optical path, the image can be conjugated either with the object plane or with the Fourier plane, thus, permitting to access both direct and reciprocal spaces.^{9,18} The guided mode was excited here using a diascope illumination with a $20\times$ objective opened at 0.35 numerical aperture. Scattering on a waveguide defect generates a continuum of wavevectors, some of them fulfilling the condition given by Eq. (1), thereby exciting the supported mode. In this case, two counterpropagating modes are excited [see Fig. 4(a)]. The polarization direction was aligned perpendicularly to the axis of the waveguide and parallel to the substrate (TE). Contrary to Fig. 1, this setup is not a measure of the reflectivity. Only the leakage radiations collected by the immersion objective will be detected and the signature of the guided mode in the Fourier plane will appear as a bright line and not as an absorption dip.

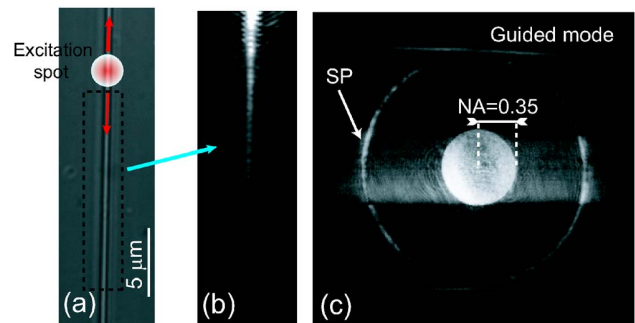


FIG. 4. (Color online) (a) Optical micrograph of the polymer waveguide fabricated on a gold substrate. Leakage radiation microscopy observations of the propagation in the waveguide: (b) imaging plane and (c) Fourier plane.

Figure 4(b) is the corresponding leakage image acquired in direct space showing the mode propagating from top to bottom inside the polymer waveguide (the excitation area is outside the field of view of the camera). An exponential fit of the intensity along the waveguide gives a propagation length $L_\alpha = 4.8 \pm 0.5 \mu\text{m}$ in good agreement with the calculated value. The intensity distribution in the waveguide demonstrates the single mode nature of the mode. This characteristic is confirmed by the reciprocal Fourier image, shown in Fig. 4(c). The signature of the guided mode appears as a single bright horizontal line in Fourier space corresponding to the propagating mode, displayed in Fig. 4(b) [two lines are present; they correspond to the two counterpropagating modes, as shown in Fig. 4(a)]. It is worth to note that these lines are the direct consequences of the field confinement of the guided mode in the transverse direction. Indeed, the Fourier transform of such a confined field distribution features necessarily a wide angular spectrum in the transverse (i.e., x axis) direction and a single value of the wavevector in longitudinal direction corresponding to the propagation constant of the guided mode. Additionally, the thin film surface plasmon excitation appears as a bright ring in the image (as a polarized beam is focused on the structure, it contains vertical components of the field allowing the excitation of a surface plasmon). The large central band simply reveals light diffraction perpendicular to the line structure. Knowing the full numerical aperture of the excitation and the collection objectives, it is easy to calibrate the image and extract $\Re(n_{\text{eff}})$ of the guided mode. From the image, a value of $\nu = 1.08 \pm 0.03$ is obtained, which is also in very good agreement with the theoretical value given by the differential method.

In conclusion, polymer waveguides lying on a metal film have been studied by using the differential method and leakage radiation microscopy in direct and reciprocal spaces. These numerical and experimental tools are providing powerful characterization of the nature of the modes propagating inside the structure. In particular, the complex effective index of the modes can be theoretically estimated and experimen-

tally determined. Fair agreements have been obtained. These techniques are well suited to characterize dielectric-loaded surface plasmon waveguides (or other structures presenting radiation losses) and to evaluate their potential for information processing devices.

The authors gratefully acknowledge S. I. Bozhevolnyi and T. Holmgaard for initial design inputs. This work was financially supported by the European Commission (PLAS-MOCOM Project EC FP6 IST 034754 STREP).

- ¹W. Barnes, A. Dereux, and T. Ebbesen, *Nature* (London) **424**, 824 (2003).
- ²T. Holmgaard and S. Bozhevolnyi, *Phys. Rev. B* **75**, 245405 (2007).
- ³A. Krasavin and A. Zayats, *Appl. Phys. Lett.* **90**, 211101 (2007).
- ⁴R. Kiyari, C. Reinhardt, S. Passinger, A. L. Stepanov, A. Hohenau, J. Krenn, and B. Chichkov, *Opt. Express* **15**, 4205 (2007).
- ⁵B. Steinberger, A. Hohenau, H. Ditlbacher, A. Stepanov, A. Drezet, F. Aussenegg, A. Leitner, and J. Krenn, *Appl. Phys. Lett.* **88**, 094104 (2006).
- ⁶B. Steinberger, A. Hohenau, H. Ditlbacher, F. Aussenegg, A. Leitner, and J. Krenn, *Appl. Phys. Lett.* **91**, 081111 (2007).
- ⁷A. Bouhelier and G. Wiederrecht, *Opt. Lett.* **30**, 884 (2005).
- ⁸A. Hohenau, J. Krenn, A. Stepanov, A. Drezet, H. Ditlbacher, B. Steinberger, A. Leitner, and F. Aussenegg, *Opt. Lett.* **30**, 893 (2005).
- ⁹M. González, A. Stepanov, J.-C. Weeber, A. Hohenau, A. Dereux, R. Quidant, and J. Krenn, *Opt. Lett.* **32**, 2704 (2007).
- ¹⁰J. Jägerskå, N. Le Thomas, R. Houdré, J. Bolten, C. Moormann, T. Wahlbrink, J. Čtyroký, M. Waldow, and M. Först, *Opt. Lett.* **32**, 2723 (2007).
- ¹¹I. Stefanon, S. Blaize, A. Bruyant, A. Aubert, G. Lerondel, R. Bachelot, and P. Royer, *Opt. Express* **13**, 5553 (2005).
- ¹²A. Snyder and J. Love, *Optical Waveguide Theory* (Chapman and Hall, London, 1983).
- ¹³M. Nevière and E. Popov, *Light Propagation in Periodic Media, Differential Theory and Design* (Dekker, New York, 2003).
- ¹⁴L. Li, *J. Opt. Soc. Am. A* **13**, 1024 (1996).
- ¹⁵J. Goodman, *Introduction to Fourier Optics* 2nd ed. (McGraw-Hill, New York, 1996).
- ¹⁶E. Palik, *Handbook of Optical Constants of Solids* (Academic, New York, 1985).
- ¹⁷B. Hecht, H. Bielefeldt, L. Novotny, Y. Inoué, and D. Pohl, *Phys. Rev. Lett.* **77**, 1889 (1996).
- ¹⁸A. Drezet, A. Hohenau, A. Stepanov, H. Ditlbacher, B. Steinberger, N. Galler, F. Aussenegg, A. Leitner, and J. Krenn, *Appl. Phys. Lett.* **89**, 091117 (2006).